GEOLOGY | THE GEOLOGICAL SOCIETY OF AMERICA®

https://doi.org/10.1130/G50131.1

Manuscript received 13 February 2022
Revised manuscript received 30 March 2022
Manuscript accepted 1 April 2022

Published online 27 May 2022

Mercury isotopic composition of igneous rocks from an accretionary orogen: Implications for lithospheric recycling

Changzhou Deng[1], Jun Gou[2]*, Deyou Sun[2], Guangyi Sun[1], Zhendong Tian[1], Bernd Lehmann[3], Frédéric Moynier[4] and Runsheng Yin[1]*

[1]State Key Laboratory of Ore Deposit Geochemistry, Institute of Geochemistry, Chinese Academy of Sciences, Guiyang 550081, China
[2]College of Earth Sciences, Jilin University, Changchun 130061, China
[3]Department of Mineral Resources, Technical University of Clausthal, Clausthal-Zellerfeld 38678, Germany
[4]Institut de Physique du Globe de Paris, Université de Paris, CNRS, Paris 75005, France

ABSTRACT

Mercury (Hg) provides critical information on terrestrial planet formation and evolution due to its unique physicochemical properties and multiform isotopic compositions. Current knowledge of Hg is mainly limited to Earth's surface environments, and the understanding of Hg in the Earth's interior remains unclear. Accretionary orogens are major settings for continental crustal growth and crust-mantle interactions. We studied the Hg concentration and isotopic composition of igneous rocks in the eastern Central Asian orogenic belt, using Hg as a proxy to trace the recycling of surface materials in Earth's lithosphere. Our results show low Hg abundances in mafic through felsic igneous rocks (4.93 ± 4.35 ppb, standard deviation [SD], $n = 267$). Mafic rocks show slightly lower δ^{202}Hg (−2.9‰ ± 0.5‰, SD, $n = 24$) than intermediate (−2.4‰ ± 0.8‰, SD, $n = 58$) and felsic (−1.5‰ ± 0.8‰, SD, $n = 185$) rocks, indicating a chemical stratification of Hg isotopic composition in the continental crust with isotopically lighter Hg in the lower part and heavier Hg in the upper part. Slightly positive Δ^{199}Hg values are observed in mantle-derived mafic (0.07‰ ± 0.06‰, SD) and intermediate (0.06‰ ± 0.07‰, SD) rocks, which agree well with those reported for marine sediments, indicating the involvement of fluids or melts from the oceanic crust. Larger variations of Δ^{199}Hg values (−0.26‰ to +0.21‰, average: 0.01‰ ± 0.08‰, SD, $n = 185$) are observed in felsic rocks, further indicating recycling of surface Hg from the marine reservoir via slab subduction (reflected by positive values) plus magmatic assimilation of terrestrial Hg (reflected by negative values). Our study demonstrates that Hg isotopes can be a promising tracer for the chemical dynamics of Earth's lithosphere.

INTRODUCTION

Mercury (Hg) is a unique metal due to its high volatility, atmospheric transport, and active redox chemistry (Selin, 2009). Mercury has seven stable isotopes (^{196}Hg, ^{198}Hg, ^{199}Hg, ^{200}Hg, ^{201}Hg, ^{202}Hg, and ^{204}Hg) and is the only metal that undergoes both significant isotopic mass-dependent fractionation (MDF, defined as δ^{202}Hg) and mass-independent fractionation (MIF, usually defined as Δ^{199}Hg; see below for calculation of δ^{202}Hg and Δ^{199}Hg). Hg-MDF occurs during chemical, physical, and biological processes, whereas Hg-MIF occurs mainly during photochemical processes near Earth's surface (Blum et al., 2014). The complementary Hg-MIF signals of terrestrial surface environments (mostly negative Δ^{199}Hg) and oceanic environments (mostly positive Δ^{199}Hg) are not significantly modified by high-temperature processes, allowing tracing of deep cycling of surface-derived Hg (Deng et al., 2021; Moynier et al., 2021; Yin et al., 2022).

Accretionary orogens are key locations for large-scale continental crustal growth and crust-mantle interactions (Hofmann, 1997; Zheng, 2019), which are associated with extensive multistage magmatism (Cawood et al., 2009; Kemp et al., 2009; Moyen et al., 2017). Igneous rocks in accretionary orogenic belts may provide critical information on Hg abundance, isotopic composition, and recycling in the lithosphere. Notably, with the recent development of a high-precision Hg isotope determination method for low-Hg samples (Moynier et al., 2020), investigating the Hg isotopic composition of igneous rocks is now possible.

We measured the Hg abundance and isotopic composition of intrusive rocks (gabbro, diorite, and granitic rocks) and extrusive rocks (basalt, andesite, dacite, and rhyolite) from the eastern part of the Central Asian orogenic belt. Our study included an extensive set of bulk rock samples from the late Neoproterozoic to Early Cretaceous that is well suited to following the evolution of this long-lasting orogen, reflecting superimposed processes of continental arc and extensional backarc magmatism with a major juvenile component of crustal growth (Şengör et al., 1993; Liu et al., 2021). Our study aims to elucidate the isotopic distribution and behavior of Hg during crustal-mantle interactions and verifies that Hg isotopes can be used as a tracer for lithospheric recycling. Different from but complementary to the more traditional radiogenic isotope tracers (Sr, Nd, Hf, Os), stable Hg isotope patterns reveal recycling pathways related to near-surface atmosphere-land-hydrosphere fractionation processes.

STUDY AREA

The east-west–trending Central Asian orogenic belt is a large Paleozoic to Mesozoic subduction-related accretionary orogen between the Siberian, Tarim, and North China cratons (Fig. 1A; Jahn, 2004). It is characterized by a long history of accretion and collision of multiple microcontinents, terranes, and arc–backarc systems (Xiao et al., 2015). The eastern part of the belt, which consists of a series

*E-mails: goujun860411@163.com; yinrunsheng@mail.gyig.ac.cn

CITATION: Deng, C., et al., 2022, Mercury isotopic composition of igneous rocks from an accretionary orogen: Implications for lithospheric recycling: Geology, v. 50, p. 1001–1006, https://doi.org/10.1130/G50131.1

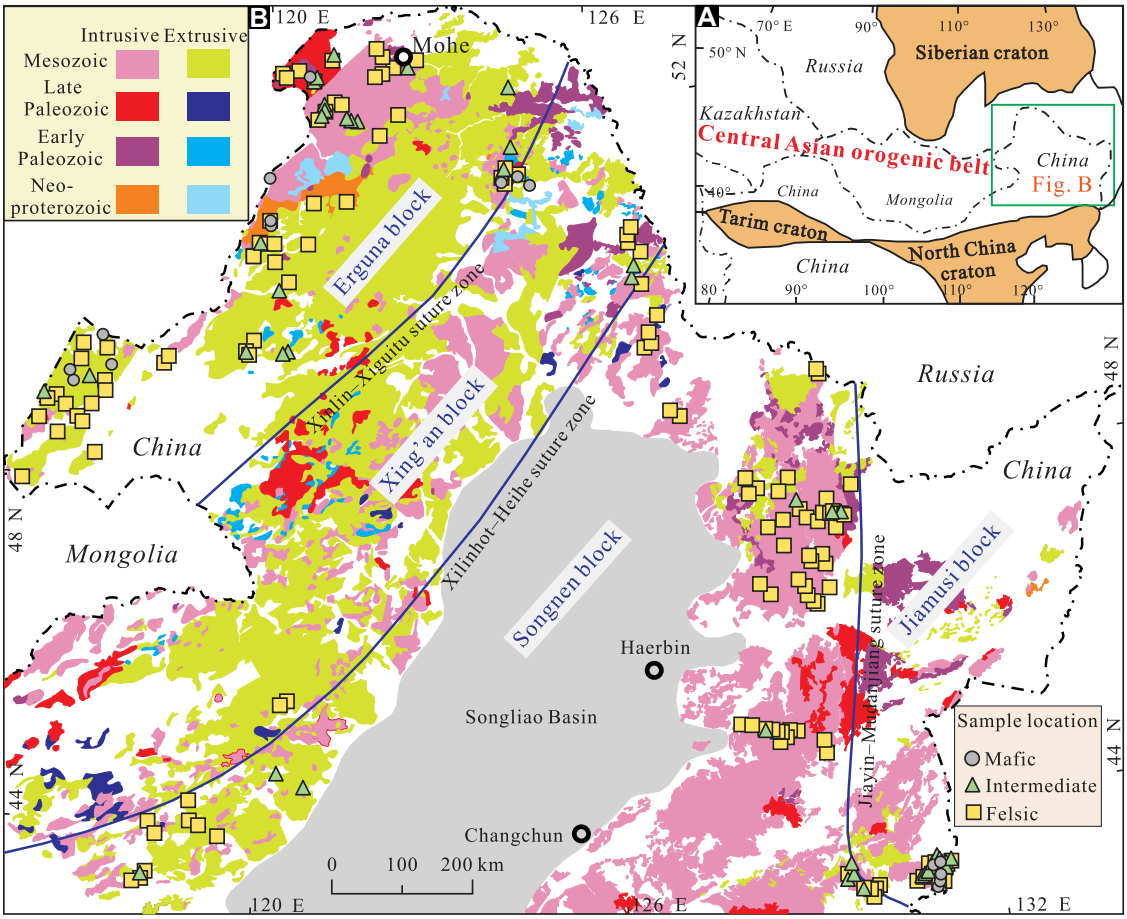

Figure 1. (A) Sketch map of the Central Asian orogenic belt and location of the studied area (after Jahn, 2004). (B) Geological map showing distribution of igneous rocks in the eastern Central Asian orogenic belt and the sampling sites of this study (after Wu et al., 2011; Xu et al., 2013).

of microcontinents, including the Erguna, Xing'an, Songnen, Jiamusi, and Wandashan blocks from west to east (Fig. 1B), underwent the subduction of the Paleo-Asian oceanic slab during the Paleozoic–early Mesozoic, the southward subduction of the Mongol-Okhotsk plate during the late Paleozoic–late Mesozoic, and the northwestward subduction of the Paleo-Pacific plate during the late Mesozoic (Wu et al., 2011). Multistage oceanic subduction formed a lithospheric mantle metasomatized by oceanic fluids or melts, and large volumes of mantle magma established a basaltic lower crust overlain by subduction-related mafic to intermediate igneous rocks (Xu et al., 2013; Deng et al., 2019). Asthenospheric upwelling caused by the foundering or rollback of the subducted paleo-oceanic slabs led to partial melting of the largely juvenile lower crust and formation of widespread felsic igneous rocks in the middle to upper crust (Wu et al., 2011; Ge et al., 2021).

SAMPLES AND METHODS

A total of 267 fresh igneous samples, including 24 mafic rocks, 58 intermediate rocks, and 185 felsic rocks, were collected from the eastern Central Asian orogenic belt (Fig. 1B); (98 samples collected during our study, and 169 collected during previous studies [see Table S1 in the Supplemental Material[1] for the sample data and references for the other studies]). The whole-rock geochemistry of 169 samples was previously reported (see Table S1 and references therein), and the additional 98 samples were analyzed here using X-ray fluorescence and inductively coupled plasma–mass spectrometry (ICP-MS). Total Hg (THg) concentrations of all samples were determined using a DMA-80 Hg analyzer. Prior to Hg isotope analysis, Hg in the sample powders was preconcentrated into 5 mL of 40% mixed acid solution (vol/vol, HNO_3/HCl = 2:1) using a double-stage combustion method (Zerkle et al., 2020). Hg-MDF is expressed in δ^{202}Hg notation in units of per mil (‰) referenced to the U.S. National Institute of Standards and Technology NIST-3133 Hg standard (analyzed before and after each sample analysis):

$$\delta^{202}\mathrm{Hg}(‰) = [(^{202}\mathrm{Hg}/^{198}\mathrm{Hg})_{\mathrm{sample}}/(^{202}\mathrm{Hg}/^{198}\mathrm{Hg})_{\mathrm{standard}} - 1] \times 1000. \quad (1)$$

[1]Supplemental Material. Samples and methods, and analytical results for igneous rocks in northeast China. Please visit https://doi.org/10.1130/GEOL.S.19783012 to access the supplemental material, and contact editing@geosociety.org with any questions.

Hg-MIF is reported in Δ notation, which describes the difference between the measured δ^{xxx}Hg and the theoretically predicted δ^{xxx}Hg value, in units of per mil (‰), where *xxx* = 199, 200, or 201:

$$\Delta^{xxx}\mathrm{Hg} \approx \delta^{xxx}\mathrm{Hg} - \delta^{202}\mathrm{Hg} \times \beta. \quad (2)$$

β is equal to 0.2520 for ^{199}Hg, 0.5024 for ^{200}Hg, and 0.7520 for ^{201}Hg (Blum and Bergquist, 2007). Detailed analytical methods are given in the Supplemental Material.

RESULTS

Total Hg (THg) contents are consistently low among mafic rocks (6.12 ± 4.86 ppb, standard deviation [SD]), intermediate rocks (6.40 ± 4.10 ppb, SD), and felsic rocks (4.31 ± 4.23 ppb, SD). δ^{202}Hg and Δ^{199}Hg values of all samples show large ranges: −4.13‰ to 0.77‰ and −0.26‰ to 0.21‰, respectively. Mafic rocks show the lowest δ^{202}Hg (−2.9‰ ± 0.5‰, SD), followed by intermediate rocks (−2.4‰ ± 0.8‰, SD) and felsic rocks (−1.5‰ ± 0.8‰, SD) (Fig. 2A). Mafic and intermediate rocks show slightly positive Δ^{199}Hg values of 0.07‰ ± 0.06‰ (SD) and 0.06‰ ± 0.07‰ (SD), respectively, whereas felsic rocks show a wider range of both positive and negative Δ^{199}Hg values (−0.26‰ to 0.21‰) (Figs. 2B and 2C).

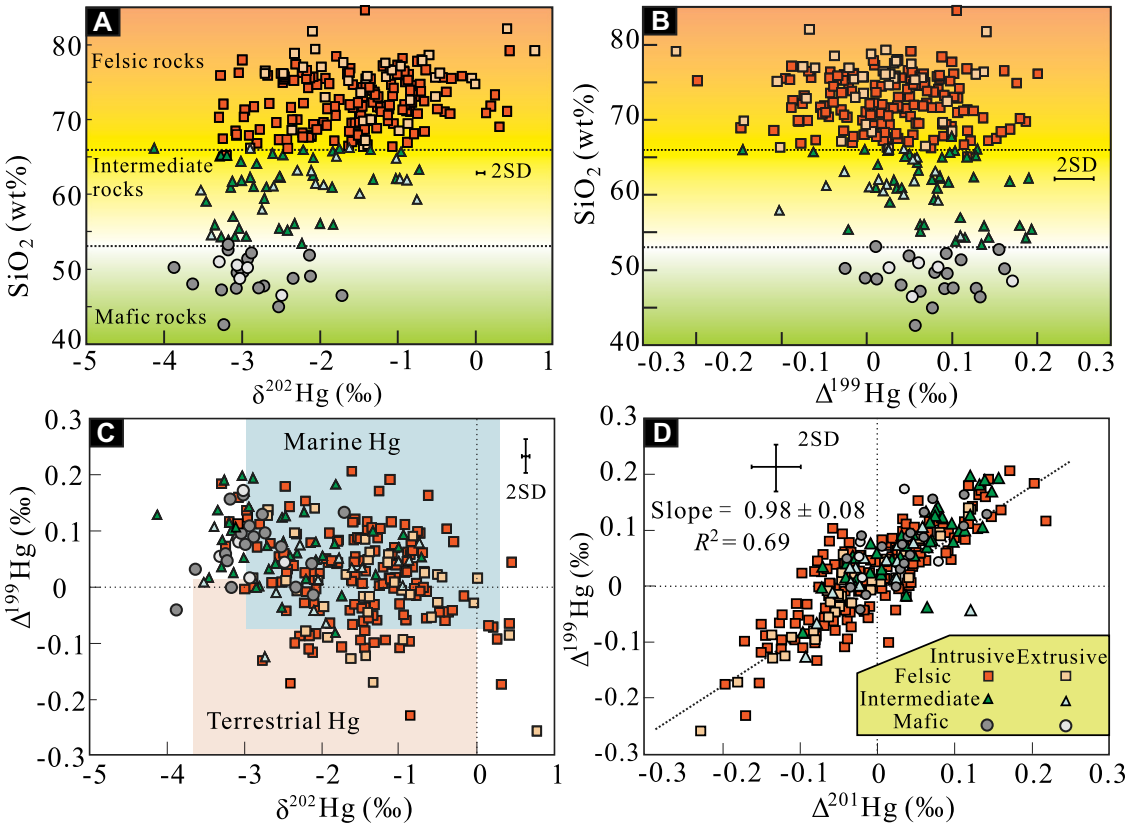

Figure 2. SiO_2 versus $\delta^{202}Hg$ (A), SiO_2 versus $\Delta^{199}Hg$ (B), $\Delta^{199}Hg$ versus $\delta^{202}Hg$ (C), and $\Delta^{201}Hg$ versus $\Delta^{199}Hg$ (D) diagrams for igneous rocks collected from the eastern Central Asian orogenic belt (compositional area of marine sediments and terrestrial Hg are after Deng et al., 2021, and references therein). SD—standard deviation.

Low whole-rock loss-on-ignition (LOI) values, the absence of correlation between LOI and THg, $\delta^{202}Hg$, or $\Delta^{199}Hg$ (Fig. S1), and the different Hg isotopic compositions between the studied rocks and hydrothermal systems (Fig. S2) exclude the influence of late-stage alteration in our samples. Though Hg isotopic data of basalts were previously reported (Moynier et al., 2021), this study expands (tenfold) the database on Hg isotopes in igneous rocks, allowing for additional constraints on the Hg isotopic composition of the lithosphere (detailed below).

DISCUSSION

Low Hg Abundance in Igneous Rocks

All samples studied show an average THg of 4.93 ± 4.35 ppb (SD), which compares well with that for the igneous rocks in the Bonanza arc, Vancouver Island, Canada (2.9 ± 2.6 ppb, SD; Canil et al., 2015). There is no significant difference in THg contents ($p < 0.05$, ANOVA) between intrusive and extrusive rocks, suggesting that igneous rocks formed at different depths of juvenile continental crust generally have low Hg contents at the parts-per-billion level. Geological reservoirs containing high Hg contents (tens of parts per billion to hundreds of parts per million Hg) mainly include low-temperature hydrothermal systems (containing Hg, Au, As, Sb, etc.) formed at shallow depths (<5 km) (Deng et al., 2021) and sedimentary rocks with high contents of organic carbon (Grasby et al., 2019), due to the affinity of Hg to sulfur and organic matter and the tendency of Hg to become enriched in low-temperature environments. The globally low THg contents of Earth's igneous rocks may relate to Hg degassing via magmatism (Zambardi et al., 2009) and/or partitioning into the core during planetary differentiation (Moynier et al., 2020). This inference is supported by the high Hg levels in volcanic gas (10–10^2 ng/m^3; Zambardi et al., 2009) and ordinary chondrite samples (1038 ± 1157 ppb, SD; Meier et al., 2016; Moynier et al., 2020). However, given that no experimental data on metal-silicate partitioning of Hg is available, future work is needed to verify this possibility.

Variation and Distribution of $\delta^{202}Hg$ in Continental Lithosphere

The large variation of $\delta^{202}Hg$ (of as much as 4.90‰) observed in this study (Fig. 2A) suggests a heterogeneous distribution of Hg isotopes in the lithosphere. The mafic and intermediate rocks have significantly negative $\delta^{202}Hg$ values (−2.5‰ ± 0.8‰, SD), consistent within error with the estimate of the composition of Earth's mantle based on data from high-$^3He/^4He$ basalts from Samoa and Iceland (−1.7‰ ± 0.6‰, SD; Moynier et al., 2021). This further implies that the mantle is likely enriched in isotopically light Hg (Moynier et al., 2020). Even some of the felsic rocks with elevated SiO_2 contents show low $\delta^{202}Hg$ values similar to that of the primitive mantle (Fig. 2A), suggesting limited Hg-MDF during partial melting and magma fractionation (Moynier et al., 2021). Volcanic gases from Vulcano island, Italy, have a $\delta^{202}Hg$ value (−1.7‰ ± 0.2‰, SD, $n = 1$; Zambardi et al., 2009) identical to that of the primitive mantle (−1.7‰ ± 0.6‰, SD; Moynier et al., 2021), implying negligible Hg-MDF during volcanic degassing. However, more data and future studies are needed to validate this inference.

The higher mean $\delta^{202}Hg$ in felsic rocks (−1.5‰ ± 0.8‰, SD) seems to reflect assimilation of upper continental crust during magma evolution, given that sediments have elevated $\delta^{202}Hg$ values of −0.68‰ ± 0.45‰ (SD; Blum et al., 2014). Such assimilation is supported by Figure 3, in which, despite a few outliers, most of the samples with higher $\delta^{202}Hg$ values ($\delta^{202}Hg > -1.0$‰) show lower concentrations of compatible elements (e.g., Ti, Fe, Mg, V, and Cr) but higher concentrations of incompatible elements which have continental crust-affinity (e.g., Si, K, and Rb). Igneous rocks from the California Coast Ranges (USA), also show high $\delta^{202}Hg$ values (−1.2‰ to −0.46‰; Smith et al., 2008), which were recently explained by crustal assimilation (Moynier et al., 2021). Considering that Earth's continental crust is chemically stratified with alumina enrichment in the upper continental crust and magnesium enrichment in the lower part, we propose here that the juvenile lower crust consisting of mafic and intermediate igneous rocks has $\delta^{202}Hg$ values of

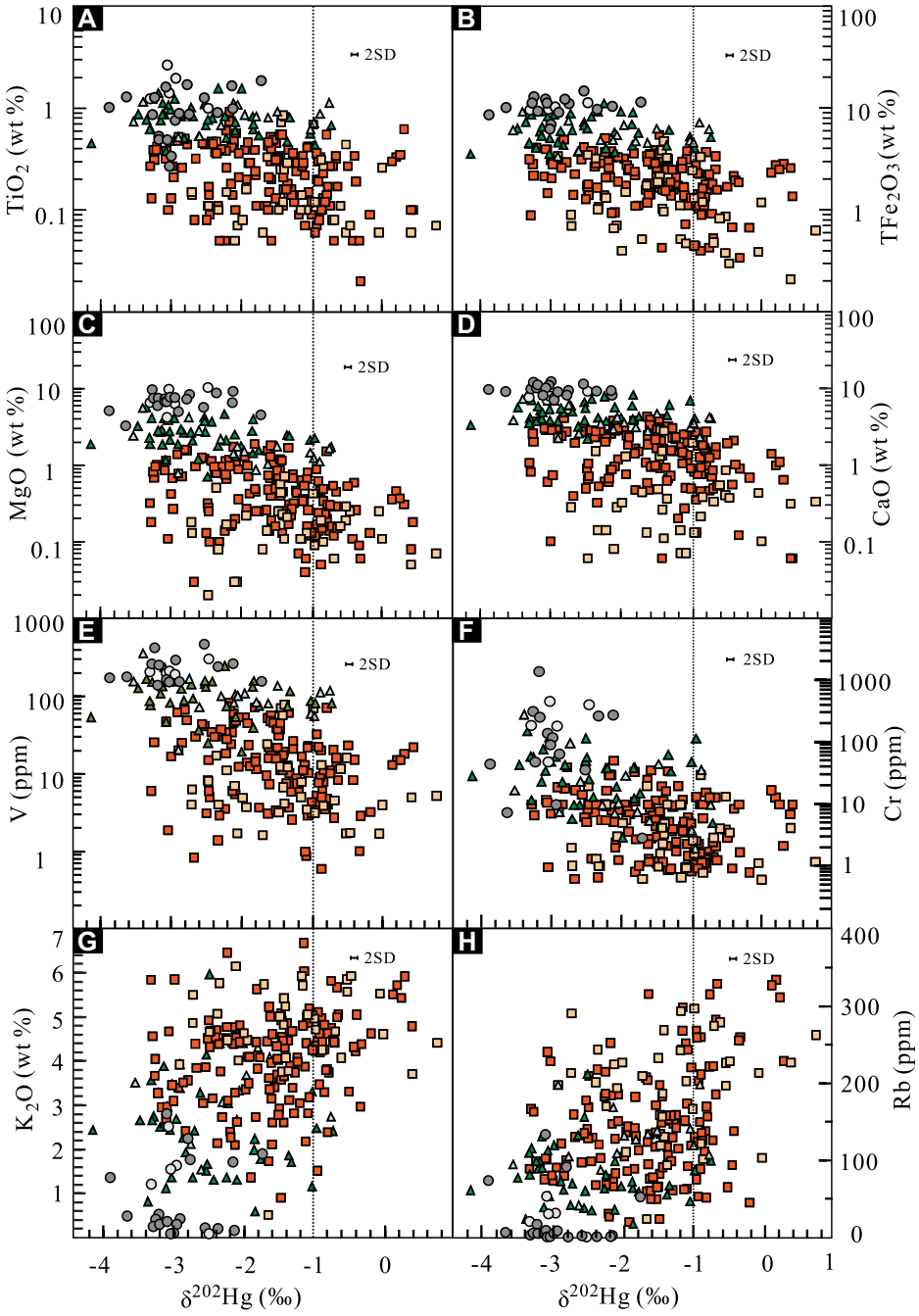

Figure 3. TiO_2 (A), total Fe_2O_3 (TFe_2O_3) (B), MgO (C), CaO (D), V (E), Cr (F), K_2O (G), and Rb (H) versus δ^{202}Hg diagrams, showing that samples with isotopically heavy Hg (δ^{202}Hg >−1.00‰) generally have low contents of compatible elements (Ti, Fe, Mg, Ca, V, Cr) and high contents of incompatible elements (K, Rb). See Figure 2 for symbol explanation. SD—standard deviation.

−2.5‰ ± 0.8‰ (SD) and that the upper continental crust consisting of felsic rocks has higher δ^{202}Hg values of −1.5‰ ± 0.8‰ (SD). Our proposal is consistent with previous inferences that Earth's interior must be more enriched in lighter Hg isotopes than surface materials (Moynier et al., 2020). We hypothesize that the δ^{202}Hg value of the continental lithospheric mantle may be higher than that of the primitive mantle (−1.7‰ ± 0.6‰, SD; Moynier et al., 2021) due to the addition of isotopically heavier Hg in sediments via oceanic slab subduction.

Mass-Independent Fractionation of Hg and Implications for Tracing Deep Recycling

In the Δ^{199}Hg versus Δ^{201}Hg diagram (Fig. 2D), all samples show a Δ^{199}Hg/Δ^{201}Hg ratio of 0.98 ± 0.08 (2SD), which is identical to that observed during aqueous Hg(II) photoreduction (Δ^{199}Hg/Δ^{201}Hg = 1.02; Bergquist and Blum, 2007). The primitive mantle has been previously hypothesized to have no Hg-MIF (Δ^{199}Hg ~0; Sherman et al., 2009; Moynier et al., 2021). On Earth's surface, Hg(II) photoreduction leads to negative Δ^{199}Hg in gaseous Hg(0) and terrestrial reservoirs (soil and vegetation), leaving positive Δ^{199}Hg in the aqueous Hg(II) species that are preferentially preserved in marine reservoirs (marine sediments and seawater; Blum et al., 2014; Jiskra et al., 2021). Given the lack of Hg(II) photoreduction in Earth's deep reservoirs, the observed Hg-MIF signal in igneous rocks should reflect the recycling of Hg from Earth's surface pools into deeper reservoirs (Moynier et al., 2021), as illustrated in Figure 4 and discussed below.

Based on analysis of ^{3}He-rich basalts, the primitive mantle is estimated to have Δ^{199}Hg close to 0‰ (Moynier et al., 2021), which is quite different from the pronounced positive Δ^{199}Hg observed in marine sediments and seawater (as high as 0.4‰; Jiskra et al., 2021). Mafic rocks studied here show positive Δ^{199}Hg values overlapping with those reported for marine sediments and seawater (Fig. 2C), suggesting recycling of Hg from marine systems into the lithospheric mantle via plate subduction (Fig. 4). This is consistent with recent studies on igneous rocks in northeastern China demonstrating that the lithospheric mantle sources of the mafic rocks were metasomatized by oceanic fluids or melts (Xu et al., 2013; Deng et al., 2019). Interestingly, continental crust–derived felsic rocks show both positive and negative Δ^{199}Hg values (Fig. 2B). The positive Δ^{199}Hg values of felsic rocks may be explained by an inherited geochemical signature from the mafic lower crust with positive Δ^{199}Hg values; however, involvement of Hg from marine strata by assimilation in the upper continental crust is more likely (Fig. 4). Negative Δ^{199}Hg values in the felsic rocks plot in the range of terrestrial reservoirs (Fig. 2C), indicating the assimilation of terrestrial materials in the magma source or during magma ascent. Such crustal assimilation is also indicated by negative zircon $\varepsilon_{Hf(t)}$ (Ge et al., 2021) and high whole-rock $^{87}Sr/^{86}Sr$ (>0.704) and low $\varepsilon_{Nd(t)}$ (<5) values of the felsic rocks in northeastern China (Deng et al., 2019, and references therein).

CONCLUSION

Our study characterizes the systematics of concentration and isotopic composition of Hg in igneous rocks from the eastern Central Asian orogenic belt, which provides new insights into the Hg isotopic composition of the continental lithosphere and Hg cycling. We suggest a depletion of Hg in Earth's igneous rocks (at the parts-per-billion level) due to Hg degassing or partitioning into the core. We propose a heterogeneous Hg isotopic composition for the continental crust: isotopically light Hg (δ^{202}Hg: −2.5‰ ± 0.8‰, SD) in the lower crust and heavier Hg (δ^{202}Hg: −1.50‰ ± 0.8‰, SD) in the upper part. Significantly positive and negative Δ^{199}Hg values (to 0.21‰ and −0.26‰,

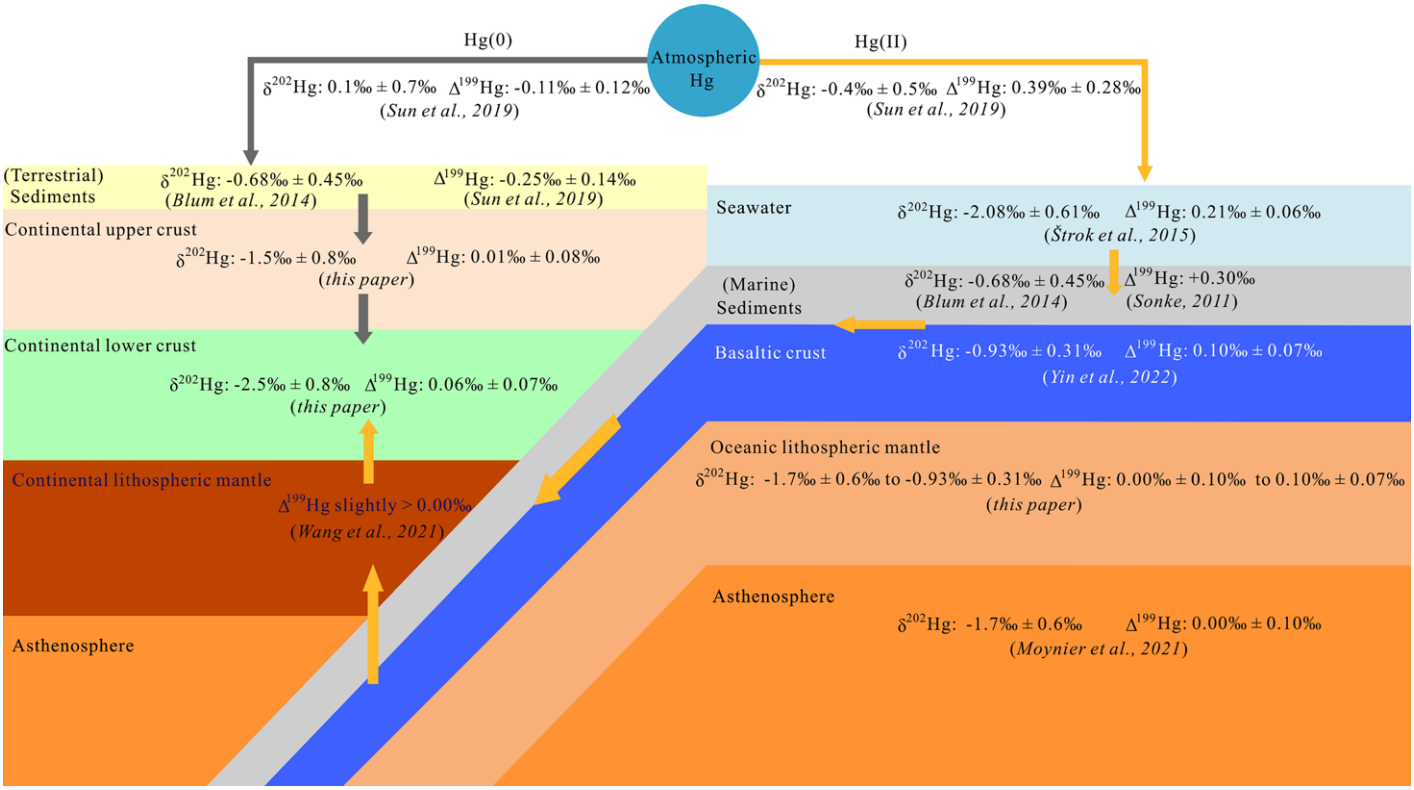

Figure 4. Proposed scenario showing isotopic composition and cycling of Hg in the atmosphere (Sun et al., 2019), seawater (Štrok et al., 2015), marine sediments (Blum et al., 2014; Sonke, 2011), basaltic crust (Yin et al., 2022), terrestrial sediments (Blum et al., 2014; Sun et al., 2019), continental crust (composed of igneous rocks; this study), and asthenospheric mantle (Moynier et al., 2021). A slightly positive Δ^{199}Hg value is attributed to the subcontinental lithospheric mantle due to metasomatism of oceanic slab fluids or melts (Wang et al., 2021). Mercury isotopic composition of oceanic lithospheric mantle is inferred here between that of the asthenosphere and that of basaltic crust.

respectively) observed in the studied igneous rocks indicate recycling via slab subduction and magmatic assimilation of surface-derived Hg affected by photochemical (atmospheric) fractionation (Fig. 4). Based on the available Hg isotopic signatures for the mantle, marine, and terrestrial end members, our new results allow us to develop a model of Hg cycling in the lithosphere. This study shows the potential of using Hg isotopes to understand the broad-scale chemical dynamics of Earth.

ACKNOWLEDGMENTS

This work was supported by the National Natural Science Foundation of China (grant 41603020). Joel D. Blum, editor Urs Schaltegger, and anonymous reviewers are thanked for their valuable comments.

REFERENCES CITED

Bergquist, B.A., and Blum, J.D., 2007, Mass-dependent and -independent fractionation of Hg isotopes by photoreduction in aquatic systems: Science, v. 318, p. 417–420, https://doi.org/10.1126/science.1148050.

Blum, J.D., and Bergquist, B.A., 2007, Reporting of variations in the natural isotopic composition of mercury: Analytical and Bioanalytical Chemistry, v. 388, p. 353–359, https://doi.org/10.1007/s00216-007-1236-9.

Blum, J.D., Sherman, L.S., and Johnson, M.W., 2014, Mercury isotopes in Earth and environmental sciences: Annual Review of Earth and Planetary Sciences, v. 42, p. 249–269, https://doi.org/10.1146/annurev-earth-050212-124107.

Canil, D., Crockford, P.W., Rossin, R., and Telmer, K., 2015, Mercury in some arc crustal rocks and mantle peridotites and relevance to the moderately volatile element budget of the Earth: Chemical Geology, v. 396, p. 134–142, https://doi.org/10.1016/j.chemgeo.2014.12.029.

Cawood, P.A., Kröner, A., Collins, W.J., Kusky, T.M., Mooney, W.D., and Windley, B.F., 2009, Accretionary orogens through Earth history, *in* Cawood, P.A., and Kröner, A., eds., Earth Accretionary Systems in Space and Time: Geological Society, London, Special Publication 318, p. 1–36, https://doi.org/10.1144/SP318.1.

Deng, C.Z., Sun, D.Y., Li, G.H., Lu, S., Tang, Z.Y., Gou, J., and Yang, Y.J., 2019, Early Cretaceous volcanic rocks in the Great Xing'an Range: Late effect of a flat-slab subduction: Journal of Geodynamics, v. 124, p. 38–51, https://doi.org/10.1016/j.jog.2019.01.012.

Deng, C.Z., Sun, G.Y., Rong, Y.M., Sun, R.Y., Sun, D.Y., Lehmann, B., and Yin, R.S., 2021, Recycling of mercury from the atmosphere-ocean system into volcanic-arc-associated epithermal gold systems: Geology, v. 49, p. 309–313, https://doi.org/10.1130/G48132.1.

Ge, M.H., Li, L., Wang, T., Zhang, J.J., Tong, Y., Guo, L., Liu, K., Feng, L., Song, P., and Yuan, J.G., 2021, Hf isotopic mapping of the Paleozoic-Mesozoic granitoids from the Jiamusi and Songnen blocks, NE China: Implications for their tectonic division and juvenile continental crustal growth: Lithos, v. 386–387, 106048, https://doi.org/10.1016/j.lithos.2021.106048.

Grasby, S.E., Them, T.R., Chen, Z.H., Yin, R.S., and Ardakani, O.H., 2019, Mercury as a proxy for volcanic emissions in the geologic record: Earth-Science Reviews, v. 196, 102880, https://doi.org/10.1016/j.earscirev.2019.102880.

Hofmann, A.W., 1997, Mantle geochemistry: The message from oceanic volcanism: Nature, v. 385, p. 219–229, https://doi.org/10.1038/385219a0.

Jahn, B.M., 2004, The Central Asian Orogenic Belt and growth of the continental crust in the Phanerozoic, *in* Malpas, J., et al., eds., Aspects of the Tectonic Evolution of China: Geological Society, London, Special Publication 226, p. 73–100, https://doi.org/10.1144/GSL.SP.2004.226.01.05.

Jiskra, M., et al.., 2021, Mercury stable isotopes constrain atmospheric sources to the ocean: Nature, v. 597, p. 678–682, https://doi.org/10.1038/s41586-021-03859-8.

Kemp, A.I.S., Hawkesworth, C.J., Collins, W.J., Gray, C.M., and Blevin, P.L., 2009, Isotopic evidence for rapid continental growth in an extensional accretionary orogen: The Tasmanides, eastern Australia: Earth and Planetary Science Letters, v. 284, p. 455–466, https://doi.org/10.1016/j.epsl.2009.05.011.

Liu, Y.J., Li, W.M., Ma, Y.F., Feng, Z.Q., Guan, Q.B., Li, S.Z., Chen, Z.X., Liang, C.Y., and Wen, Q.B., 2021, An orocline in the eastern Central Asian Orogenic Belt: Earth-Science Reviews, v. 221, 103808, https://doi.org/10.1016/j.earscirev.2021.103808.

Meier, M.M.M., Cloquet, C., and Marty, B., 2016, Mercury (Hg) in meteorites: Variations in abundance, thermal release profile, mass-dependent and mass-independent isotopic fractionation: Geochimica et Cosmochimica Acta, v. 182, p. 55–72, https://doi.org/10.1016/j.gca.2016.03.007.

Moyen, J.-F., Laurent, O., Chelle-Michou, C., Couzinié, S., Vanderhaeghe, O., Zeh, A., Villaros, A., and Gardien, V., 2017, Collision vs.

subduction-related magmatism: Two contrasting ways of granite formation and implications for crustal growth: Lithos, v. 277, p. 154–177, https://doi.org/10.1016/j.lithos.2016.09.018.

Moynier, F., Chen, J.B., Zhang, K., Cai, H.M., Wang, Z.C., Jackson, M.G., and Day, J.M.D., 2020, Chondritic mercury isotopic composition of Earth and evidence for evaporative equilibrium degassing during the formation of eucrites: Earth and Planetary Science Letters, v. 551, 116544, https://doi.org/10.1016/j.epsl.2020.116544.

Moynier, F., Jackson, M.G., Zhang, K., Cai, H.M., Halldórsson, S.A., Pik, R., Day, J.M.D., and Chen, J.B., 2021, The mercury isotopic composition of Earth's mantle and the use of mass independently fractionated Hg to test for recycled crust: Geophysical Research Letters, v. 48, https://doi.org/10.1029/2021GL094301.

Selin, N.E., 2009, Global biogeochemical cycling of mercury: A review: Annual Review of Environment and Resources, v. 34, p. 43–63, https://doi.org/10.1146/annurev.environ.051308.084314.

Şengör, A.M.C., Natal'in, B.A., and Burtman, V.S., 1993, Evolution of the Altaid tectonic collage and Paleozoic crustal growth in Eurasia: Nature, v. 364, p. 299–307, https://doi.org/10.1038/364299a0.

Sherman, L.S., Blum, J.D., Nordstrom, D.K., McCleskey, R.B., Barkay, T., and Vetriani, C., 2009, Mercury isotopic composition of hydrothermal systems in the Yellowstone Plateau volcanic field and Guaymas Basin sea-floor rift: Earth and Planetary Science Letters, v. 279, p. 86–96, https://doi.org/10.1016/j.epsl.2008.12.032.

Smith, C.N., Kesler, S.E., Blum, J.D., and Rytuba, J.J., 2008, Isotope geochemistry of mercury in source rocks, mineral deposits and spring deposits of the California Coast Ranges, USA: Earth and Planetary Science Letters, v. 269, p. 399–407, https://doi.org/10.1016/j.epsl.2008.02.029.

Sonke, J.E., 2011, A global model of mass independent mercury stable isotope fractionation: Geochimica et Cosmochimica Acta, v. 75, p. 4577–4590, https://doi.org/10.1016/j.gca.2011.05.027.

Štrok, M., Baya, P.A., and Hintelmann, H., 2015, The mercury isotope composition of Arctic coastal seawater: Comptes Rendus Geoscience, v. 347, p. 368–376, https://doi.org/10.1016/j.crte.2015.04.001.

Sun, R.Y., Jiskra, M., Amos, H.M., Zhang, Y.X., Sunderland, E.M., and Sonke, J.E., 2019, Modelling the mercury stable isotope distribution of Earth surface reservoirs: Implications for global Hg cycling: Geochimica et Cosmochimica Acta, v. 246, p. 156–173, https://doi.org/10.1016/j.gca.2018.11.036.

Wang, X.Y., Deng, C.Z., Yang, Z.Y., Zhu, J.J., and Yin, R.S., 2021, Oceanic mercury recycled into the mantle: Evidence from positive δ^{199}Hg in lamprophyres: Chemical Geology, v. 584, 120505, https://doi.org/10.1016/j.chemgeo.2021.120505.

Wu, F.Y., Sun, D.Y., Ge, W.C., Zhang, Y.B., Grant, M.L., Wilde, S.A., and Jahn, B.M., 2011, Geochronology of the Phanerozoic granitoids in northeastern China: Journal of Asian Earth Sciences, v. 41, p. 1–30, https://doi.org/10.1016/j.jseaes.2010.11.014.

Xiao, W.J., Windley, B.F., Sun, S., Li, J.L., Huang, B.C., Han, C.M., Yuan, C., Sun, M., and Chen, H.L., 2015, A tale of amalgamation of three Permo-Triassic collage systems in Central Asia: Oroclines, sutures, and terminal accretion: Annual Review of Earth and Planetary Sciences, v. 43, p. 477–507, https://doi.org/10.1146/annurev-earth-060614-105254.

Xu, W.L., Pei, F.P., Wang, F., Meng, E., Ji, W.Q., Yang, D.B., and Wang, W., 2013, Spatial-temporal relationships of Mesozoic volcanic rocks in NE China: Constraints on tectonic overprinting and transformations between multiple tectonic regimes: Journal of Asian Earth Sciences, v. 74, p. 167–193, https://doi.org/10.1016/j.jseaes.2013.04.003.

Yin, R.S., et al., 2022, Mantle Hg isotopic heterogeneity and evidence of oceanic Hg cycling into the mantle: Nature Communications, v. 13, 948, https://doi.org/10.1038/s41467-022-28577-1.

Zambardi, T., Sonke, J.E., Toutain, J.P., Sortino, F., and Shinohara, H., 2009, Mercury emissions and stable isotopic compositions at Vulcano Island (Italy): Earth and Planetary Science Letters, v. 277, p. 236–243, https://doi.org/10.1016/j.epsl.2008.10.023.

Zerkle, A.L., Yin, R.S., Chen, C.Y., Li, X.D., Izon, G.J., and Grasby, S.E., 2020, Anomalous fractionation of mercury isotopes in the Late Archean atmosphere: Nature Communications, v. 11, 1709, https://doi.org/10.1038/s41467-020-15495-3.

Zheng, Y.F., 2019, Subduction zone geochemistry: Geoscience Frontiers, v. 10, p. 1223–1254, https://doi.org/10.1016/j.gsf.2019.02.003.

Printed in USA